ELM-like Events Excited by the Off-axis-fishbone Mode in the DIII-D Advanced Tokamak Regime

M. Okabayashi[1], G. Matsunaga[2], J.R. Ferron[3], J.S. deGrassie[3], J.M. Hanson[4], W.W. Heidbrink[5], C.T. Holcomb[6], Y. In[7], G.L. Jackson[3], M.J. Lanctot[6], R.J. La Haye[3], Y.Q. Liu[8], T.C. Luce[3], D.C. Pace[3], W.M. Solomon[1], E.J. Strait[3], A.D. Turnbull[3], F. Turco[4], and M.A. Van Zeeland[3]

[1]*Princeton Plasma Physics Laboratory, Princeton, New Jersey, USA*
[2]*Japan Atomic Energy Agency, Naka City, Ibaraki, Japan*
[3]*General Atomics, San Diego, California, USA*
[4]*Columbia University, New York, New York, USA*
[5]*University of California Irvine, Irvine, California, USA*
[6]*Lawrence Livermore National Laboratory, Livermore, California, USA*
[7]*FAR-TECH, Inc., San Diego, California, USA*
[8]*Euratom/CCFE Fusion Association, Culham Science Centre, Abingdon, UK*

The high confinement of energetic particles EP (alphas, neutral beam injected ions, RF-heated ions) is required for a fusion reactor in order to achieve high fusion gain and preserve the integrity of the first wall. The interaction of EPs with plasma instabilities [1] can have an impact on the confinement of the fast ions, their losses to the walls and global plasma performance. On the other hand, EPs are a significant contributor to the kinetic stabilization of the resistive wall mode (RWM) [2]. However, under certain conditions, EPs in DIII-D and JT-60U can excite bursting modes such as the off-axis-fishbone mode (OFM), which is similar to the classical fishbone mode, but is located near the q=2 surface and can induce the onset of the RWM [3,4].

Recent high beta plasmas in DIII-D have shown that EP-driven OFMs also trigger edge localized modes (ELM)-like events causing massive wall material (carbon) influx that prevents sustained long duration high-beta performance. Here, we use the term "ELM-like", since the D_α emission seems like typical ELM behavior. The onset of a strongly non-sinusoidal mode-distortion coincides with ELM-like event. The density perturbation observed by the CO_2 interferometer and magnetic probe signals suggest this mode distortion is a kind of "electron density snake". Excitation of ELMs by the OFM was first reported in JT-60U long duration high-beta plasmas [4].

The plasma studied in this experiment is a D-shaped single null divertor configuration

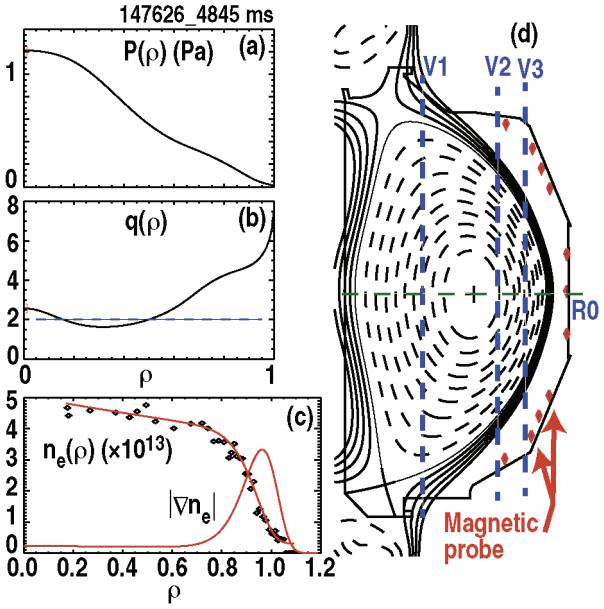

Fig. 1. Equilibrium of #147626 at 4845 ms: (a) the total plasma pressure, (b) q-profile, (c) electron density profile and the density gradient $dn_e(\rho)/d\rho$ (x10) and (d) EFIT equilibrium, with CO_2 interferometer arrays (R0, V1, V2, V3).2

with off-axis-neutral beam injection (NBI) to produce broader current- and pressure-profiles. The plasma pressure was well above the no-wall beta limit. The q-profile was flat or slightly inverted with $q_{min} \sim 1.5$ (Fig. 1) [5]. The direction of the plasma current and the toroidal field was chosen to minimize the trapped-EPs fraction with off-axis NBI, reducing the trapped partcle drive for EP-driven modes. Nonetheless, OFMs were excited as discussed here.

ELM-like behavior and carbon influx by off-axis-fishbone modes

Figure 2 shows a series of compound OFM bursts. The fundamental frequency of the OFM was ~13 kHz and the mode-distortion was synchronized in phase with the fundamental. It is interesting to note that the first crash in each compound event induced an ELM-like event resulting in massive wall material (carbon) influx. The C-III emission increased by more than one order of magnitude at the final compound event. The first crash in each such occurrence coincided with the neutron emission rate decrease [Fig. 1(c)]. In the third compound event, the rate decrease was substantial.

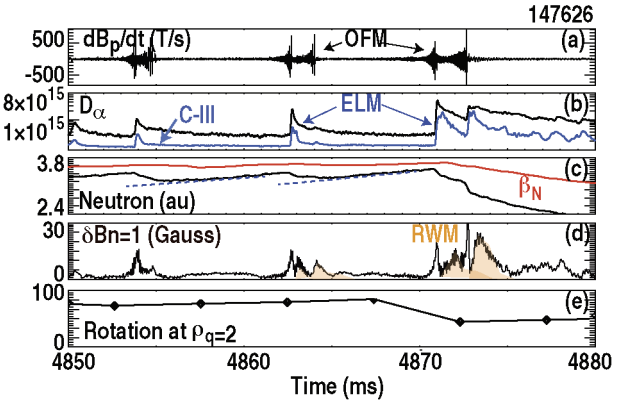

Fig. 2. Double off-axis-fishbone event (147626): (a) magnetic probe, (b) D_α and CIII, (c) neutron flux, (d) n=1 δB_p, and (e) plasma rotation at q~2.

An n=1 kink like RWM with near zero frequency was observed after the second OFM crash in each compound event. The amplitude of the RWM-like mode became larger with the third compound event, and reached 10–30 gauss, but, the time duration was brief ≈2–4 ms, implying there are strong damping mechanisms. One possibility is that the plasma rotation near the q=2 surface remained high as shown in Fig. 2(e), contributing a stabilizing effect.

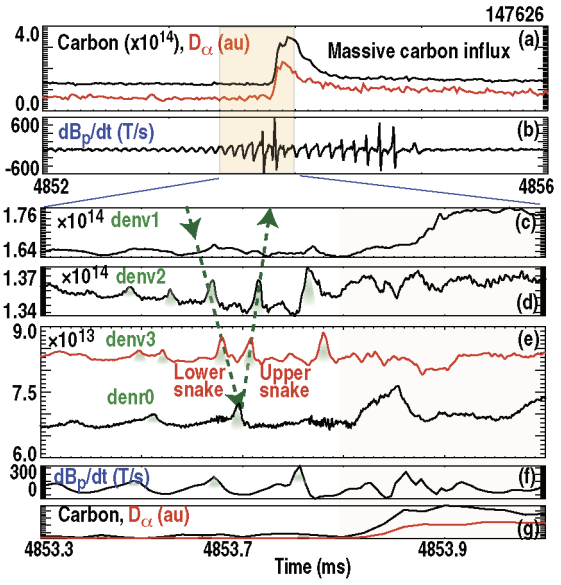

Fig. 3. ELM onset: (#147626, 4852–4856 ms), (a) D_α and CIII emission, (b) magnetic probe, 4853.5–4854.0 ms (ce) CO_2 interferometer signals (V1, V2, V3, R0), (f) magnetic probe, and (g) D_α and CIII emission.

Ideal MHD electron density snake

A question arises about possible causes of the ELM-like event. A clue is provided from the perturbed electron density observed with the CO_2 interferometer system. Figure 3 shows the perturbed electron density after the lower frequency components including the fundamental were filtered. The arrangement of the CO_2 array is shown in Fig. 1(d): one chord is on the midplane viewing horizontally (R0), others are aligned vertically slicing through various major radii (the radius of V1, V2 and V3 channels are at R=1.48 m, 1.94 m and 2.10 m respectively).

The burst observed on the midplane (R0) shows one single event, but, vertical chords show two bursting events, where the separation in time is longer for arrays located farthest away from the outboard edge. The time interval between the two bursts is due to two appearances of the helically tilted disturbance crossing the vertical viewing array. The burst was weak at the chord farther away from the outboard edge (V1) suggesting that the burst has a ballooning character. Possible mode propagation is provided by connecting peaks as shown in Fig. 3(c-e). The mode behaves like a "snake" propagating poloidally. Since the CO_2 interferometer and magnetic pickup sensor are separated toroidally, it is difficult to relate precisely the toroidal phase between these density and magnetic probe signals.

Density snake and magnetic distortion on poloidal magnetic sensor signals

The interferometer observes an integral, S_{obs}, of the perturbed electron density, δn_e, due to the mode disturbance ξ_n;

$$S_{obs} = \int \delta n_e dl \quad , \qquad \delta n_e = \xi_n \nabla n_e(\rho) \quad .$$

As shown in Fig. 1(c), the density profile $n_e(\rho)$ in the present configuration is flat inside $\rho<0.8$ and the maximum density gradient $\nabla n_e(\rho)$ occurs near $\rho\sim0.95$. Thus, the observed integral of density perturbation represents the mode behavior dominantly near the outboard edge assuming no mode compressibility. For qualitative discussion, we introduce an average quantity

$$\langle \xi_n \rangle \equiv S_{obs} / \int \nabla n_e dl = S_{obs} / \langle n_{e\nabla n} \rangle \quad ,$$

where $\langle n_{e\nabla n} \rangle$ is the average of the density in the steep gradient region. Figure 4(a) shows the CO_2 array signals (after low frequency is filtered) versus time. For each channel of CO_2 interferometer, the z-position at $\rho\sim0.85$ is used as the mode z-location, with the same trace being repeated to represent the upper/lower positions. The toroidally-localized burst propagates poloidally from bottom to the top like a snake. This propagation matches with the propagation of the mode distortion observed by poloidal magnetic probes located vertically at the outboard major radius side [locations shown in Fig. 1(d)]. The amplitude of time-integrated magnetic probe signals increases monotonically with the density distortion amplitude. The polarity of integrated magnetic probe signals agrees well with a model of a perturbed current filament with the polarity in the same direction as the plasma current, indicating that the distortion is due to simple displacement of magnetic surfaces. These observations suggest that this snake is an ideal MHD structure composed of many high-n components [6].

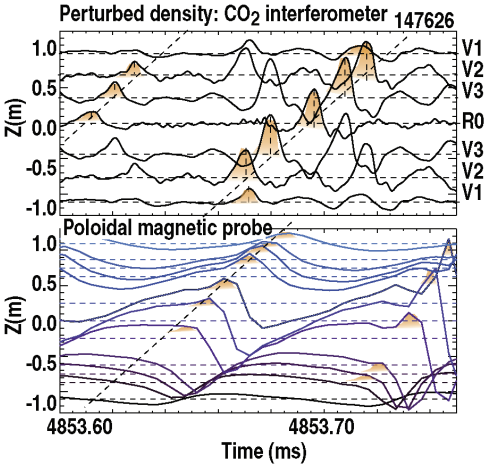

Fig. 4. (a) CO_2 interferometer signal vs time with vertical axis of z-location at ρ=0.85 along reach array (#147626). The dotted line shows the burst propagates in the poloidal direction. (b) Poloidal magnetic array signals. The dotted line is the mode propagation velocity same as shown in (a).

Figure 5 shows the time evolution of the snake amplitude before the ELM-like event. The amplitude of all interferometer chords (R0, V3, and V2) except for the one far away from the outboard edge (V1) grew rapidly before the ELM-like event. Here, the averaged displacement, $\langle \xi_n \rangle$, was increased from less than 1 cm up to ~5 cm on the ideal MHD time scale. Then, the amplitude saturated and decreased rapidly with the ELM-like event, supporting a hypothesis that the snake is responsible for the onset of the ELM-like event. The amplitude at the fundamental frequency is to be reduced in the time period of the second OFM even when stronger snake like behavior persisted (Fig. 3).

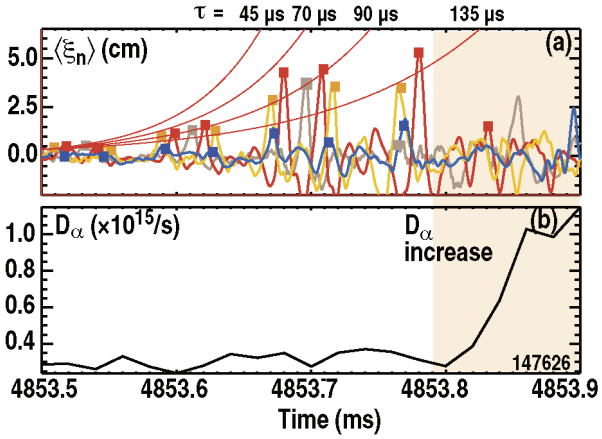

Fig. 5 (a) the average displacement evolution determined from CO_2 interferometers vs time (#147626): R0 (brown), V1 (blue), V2 (orange), and V3 (red). Possible mode growth with various τ's are overplotted. (b) D_α vs time.

These results imply that there are two phases: one with a fundamental frequency and the other a snake without fundamental. The OFM with the fundamental frequency is consistent with an external kink mode in Ref. [3]. The identification of the other phase needs further analysis such as the dependence of NBI injection angle/power to assess the reproducibility of snake formation process. Here, EPs may play a significant role for the fundamental of OFM, the formation of snake and the consequence of massive carbon influx.

This work was supported in part by the US Department of Energy under DE-AC02-09CH11466, DE-FC02-04ER54698, DE-FG02-04ER54761, SX-G903402, DE-AC52-07NA27344, and DE-FG02-08ER85195. We are thankful to Dr. E. Fredrickson who provided valuable suggestions regarding classical fishbone and snake behavior. We also express thanks to Dr. R. Nazikian who encouraged us to pursue the study of the off-axis-fishbone-driven RWM/ELM in DIII-D.

[1] W.W. Heidbrink, Phys. Plasmas **15**, 055500 (2008).
[2] B. Hu and R. Betti, Phys. Rev. Lett. **93**, 105002 (2004).
[3] M. Okabayashi, *et al.*, Phys. Plasmas **18**, 056112 (2011).
[4] G. Matsunaga, *et al.*, Nucl. Fusion **50**, 084003 (2010).
[5] C.T. Holcomb, *et al.*, Bull. Am. Phys. Soc. **56**, 97 (2011).
[6] W. Park, E. Fredrickson, *et al.*, Phys. Rev. Lett. **75**, 1765 (1995).